ESR Study on Diffusion-Controlled Atom Transfer Radical Polymerization of Methyl Methacrylate and Ethylene Glycol Dimethacrylate

Aileen R. Wang and Shiping Zhu*

Department of Chemical Engineering, McMaster University, 1280 Main Street West, Hamilton, Ontario, Canada L8S 4L7

Received July 15, 2002; Revised Manuscript Received October 21, 2002

ABSTRACT: An electron spin resonance (ESR) spectrometer was applied on-line to the atom transfer radical polymerization (ATRP) of methyl methacrylate (MMA) and ethylene glycol dimethacrylate (EGDMA) initiated by methyl α-bromophenylacetate (MBPA) with copper bromide (CuBr) and 1,1,4,7,-10,10-hexamethyltriethylenetetramine (HMTETA) as catalyst and ligand. The Cu(II) ESR signal was observable from the very beginning of the polymerization. The methacrylate radical spectrum appeared at a later stage due to the network formation of the system that imposed diffusion limitations on the fast radical deactivation and termination reactions. The radical and Cu(II) concentrations were measured and analyzed. The polymerization process appeared to have three definable stages. In the first stage, the Cu(II) concentration increased continuously but slowly. The methacrylate radical signal was not detectable because its concentration was below the sensitivity of the ESR machine. In the second stage, the Cu(II) concentration increased dramatically. The methacrylate radical signal started to appear and increased synchronously with the Cu(II) concentration. The autoacceleration was because the radical deactivation became diffusion-controlled. In the third stage, the Cu(II) and radical concentrations increased gradually and reached a steady state due to radical trapping in the network. The observation of the radical intermediate in ATRP further supported the radical mechanisms proposed for the transition-metal-mediated polymerization. The effects of comonomer composition, catalyst and initiator concentrations, and temperature on the radical concentration profiles were examined. The gel fraction, not the monomer conversion, determined the onset of the radical accumulation in this cross-linking ATRP system.

Introduction

Controlled/living radical polymerization has attracted much attention in recent years due to its potential for developing new polymer products.[1,2] Living polymerization offers good control over chain properties and functionalities and enables the preparation of tailor-made polymer materials. Compared to living anionic and cationic processes, controlled radical polymerization has the advantages of versatility of monomer types, tolerance of impurities, and mild reaction/operation conditions.

A polymerization system is considered to be living as long as there are no permanent termination and/or transfer reactions of propagating chains.[3] In general, radical (unpaired electron) species are extremely active. The livingness of a radical process relies on frequent and temporary capping/deactivation of propagating radicals during polymerization. There are three major radical capping mechanisms developed. Nitroxide-mediated polymerization (also called stable free-radical polymerization, SFRP) uses stable nitroxide radicals, such as 2,2,6,6-tetramethylpiperidinyl-1-oxy (TEMPO), as the radical deactivator.[4,5] Transition-metal-mediated polymerization (mechanistically termed as atom-transfer radical polymerization or ATRP) employs halogen atom (mainly Br and Cl) for radical capping.[6,7] Reversible addition−fragmentation transfer polymerization or RAFT uses dithioester as the radical deactivator.[8,9]

The radical capping reaction must be reversible for living process. The capped dormant chains are in equilibrium with propagating radicals. The key requirement for a radical process to be living is a rapid capping to avoid permanent radical termination. The capping rate is usually many orders of magnitude higher than that of radical uncapping/activation. Any factor that impedes the capping reaction may decrease the livingness. Diffusion limitations experienced by radical species and/or capping agents are one of the major factors. This is particularly true at high conversions when both polymer concentration and molecular weight are high and the system becomes viscous. Indeed, experimental work in the literature seldom report conversions over 90%. The lack of molecular weight control at high conversions limits the commercialization of the living radical processes. Monomer residue, even a small percentage, yields high costs for separation and recycling in industrial practices.

Diffusion control is particularly sensitive to fast reactions. Such reactions in a living radical polymerization include radical termination and deactivation. The rate constant of a diffusion-controlled reaction is proportional to the sum of the self-diffusivities of the reactants involved. Polymer diffusion is usually chain length dependent with longer chains being slower. The radical termination involves two chain species and thus readily becomes diffusion-controlled. The diffusion-controlled termination promotes livingness and thus the control over molecular weight development. The radical deactivation involves one chain species and the other small molecule, for example catalyst/ligand complex in ATRP. The diffusion-controlled deactivation rate constant is thus determined by the size of the complex. At a high conversion when the complex experiences difficulty in diffusing, the deactivation reaction becomes diffusion-controlled. In contrast to termination, the

* To whom correspondence should be addressed: e-mail zhuship@mcmaster.ca; Fax 1(905)521-1350.

10.1021/ma0211277 CCC: $22.00
Published on Web 12/02/2002

diffusion-controlled deactivation makes the polymerization system suffer from the loss of its livingness.

Radical concentrations in typical free radical polymerization processes are about $10^{-9}-10^{-7}$ mol/L, which are difficult to detect by any means. The diffusion-controlled radical reactions increase the radical concentrations to a level that can be observed. Recently, Yu et al. used electron spin resonance spectroscopy (ESR) to investigate the ATRP of poly(ethylene glycol) dimethacrylate.[10] The radical intermediates involved in the polymerization process were observed for the very first time. The cross-linking nature of the dimethacrylate system imposed severe diffusion limitations for the reacting species and triggered the buildup of radical concentration. The radical signals were very clear with their hyperfine structures typical of methacrylate radicals. The work supported the radical mechanisms proposed for the transition-metal-mediated polymerization.[11]

In this work, we carried out a systematical experimental investigation on the ATRP of methyl methacrylate (MMA) and ethylene glycol dimethacrylate (EGDMA). The objectives are threefold: The first is to provide a fundamental understanding about the radical mechanisms involved in ATRP, particularly the radical/dormant equilibrium reactions. The second is to provide insight into the diffusion limitations in ATRP processes that have implications for high-conversion controlled radical polymerization. The third is to quantify, whenever possible, the effects of the diffusion control on various reaction rates. Tremendous effort has been made in developing various polymer products using ATRP approaches since its discovery in 1995.[1,2] However, the mechanistic studies are still lacking in certain aspects. Many fundamental questions remain unanswered. The radical nature and concentration that ESR can provide are most important for the mechanistic studies. In this work, we choose the most studied MMA as a model system. Different concentrations of EGDMA as cross-linking agent are used to simulate the levels of diffusion limitations. The initiator methyl α-bromophenylacetate (MBPA), catalyst Cu(I)Br, and ligand 1,1,4,7,10,10-hexamethyltriethylenetetramine (HMTETA) are also common agents used in ATRP.

Experimental Section

Materials. Methyl methacrylate (MMA) and ethylene glycol dimethacrylate (EGDMA) from Aldrich were distilled over CaH_2 and stored at 0 °C prior to use. Copper(I) bromide (98%), methyl α-bromophenylacetate (MBPA, 97%), and 1,1,4,7,10,-10-hexamethyltriethylenetetramine (HMTETA, 97%) were all purchased from Aldrich and used as received. The solvent of acetone (laboratory grade, Caledon) and methanol (GR ACS, Merck) were also used as received. 2,2′-Azobis(2-methylpropionitrile) (AIBN, Aldrich) was recrystallized three times from absolute methanol. 4-Hydroxy-2,2,6,6-tetramethylpipieridine-1-oxy (TEMPO 98%, Sigma) was used as received.

Sample Preparation. Take the MMA/EGDMA 94.2/5.8 (vinyl based mol/mol) as a synthesis example. 0.50 mL of MMA (4.67 mmol of vinyl group), 0.027 mL of EGDMA (0.29 mmol of vinyl group), 7.3 mg of CuBr (0.05 mmol), and 13.9 μL of HMTETA (0.05 mmol) were added into a dry ampule (5 mm o.d., 3.3 mm i.d.) The ampule was then sealed with a rubber septum and bubbled with ultrahigh-purity nitrogen for 15 min. MBPA 8 μL (0.05 mmol) was added by a degassed syringe, and the ampule was shaken for 1 min prior to the ESR measurement.

ESR Measurement. An on-line electron spin resonance (ESR) measurement was carried out on a Bruker EPR spectrometer (EP072). The ESR spectrometer was operated at 0.504 mW power and 100 kHz of modulation frequency. The polymerization took place when the ampule was inserted into the EPR cavity with its temperature maintained at the preset level by a Bruker variable temperature unit. The EPR spectra were recorded at different time intervals during the polymerization.

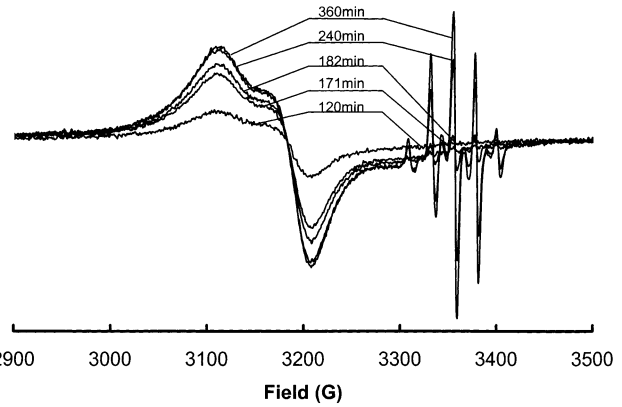

Figure 1. ESR spectra recorded during the bulk ATRP of MMA/EGDMA at 70 °C: [MMA]/[EGDMA]/[MBPA]/[Cu(I)Br]/[HMTETA] = 94.2/5.8/1/1/1 (vinyl based mol/mol). The ESR operation parameters are as follows: power 0.504 mW, microwave frequency 9.41 GHz, modulation frequency 100 kHz, modulation amplitude 3.0 G, gain 5.02×10^5, time constant 10.24 s, center field 3360 G, sweep width 800 G, resolution 1024, and the polymerization times as indicated.

The radical and Cu(II) signals were slightly overlapped, which provides a challenge for calculating their concentrations. The radical and Cu(II) concentrations were calibrated by their signal intensities. A toluene solution of TEMPO was used as a reference for the methacrylate radical. Copper(II) trifluoroacetylacetonate (Aldrich) in toluene was used for the Cu(II) species. The TEMPO spectrum is different from that of methacrylate radical. The calibration of the methacrylate radical with TEMPO must be determined by comparing the area data through double-integrating their respective spectra. For this purpose, a series of "standard" MMA/EGDMA samples were prepared by conventional free-radical polymerization using AIBN as initiator. These spectra were free of the Cu(II) signal overlapping. The radical concentrations of these "standard" samples were first calibrated with the TEMPO reference through double integration of their spectra. The radical concentrations of the ATRP samples were then obtained by comparing their intensities (the height of central line) to those of the methacrylate "standards". In the Cu(II) concentration calibration, the Cu(II) spectra at the beginning of the ATRP (before the appearance of the radical signal) were used as the "standards" for the signal area−height relationship.

Measurement of Monomer Conversion and Gel Fraction. The sample preparation is the same as that of the ESR measurement. The ampule was put into an oil bath at the preset temperature for a required time period. The reaction was stopped by immediately immersing the ampule into an ice−water bath. The ampule was broken, and the product was taken out and ground into powder. The powder was acetone-extracted in a glass beaker with vigorous stirring for 72 h. The sol polymer was recovered by precipitation in methanol. Both sol and gel polymers were dried in a vacuum oven at room temperature to a constant weight. The conversion of total monomer was determined by a gravimetrical method. The gel fraction was determined by $f_g = w_g/w_p$, where w_g is the dried gel polymer weight and w_p is the total dried polymer weight. The total monomer conversion was determined by a mass balance between the total polymer collected and the monomer amount initially charged to the ampule.

Results and Discussion

Evolution of Paramagnetic Species. Figure 1 shows the ESR spectra recorded during the bulk ATRP of MMA/EGDMA (94.2/5.8 mol/mol based on vinyl

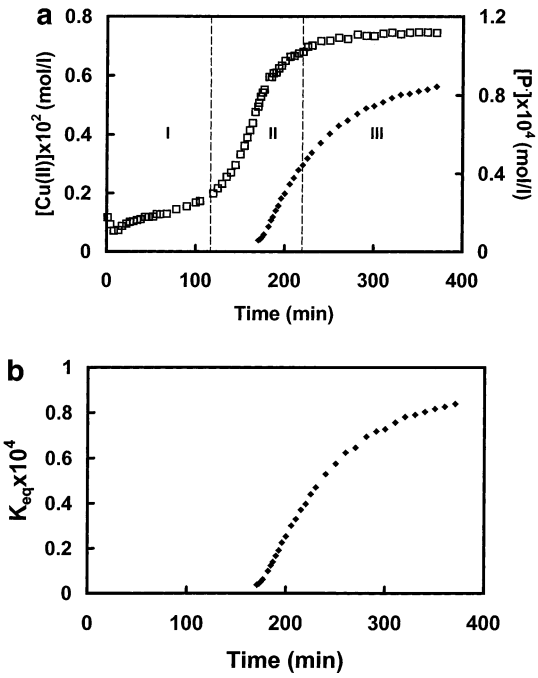

Figure 2. (a) Cu(II) and radical concentrations and (b) equilibrium constant $K_{eq} = k_{act}/k_{dea}$. The polymerization conditions are the same as in Figure 1.

group, 97/3 mol/mol on molecular base, 70 °C). At the early stage of the polymerization, the signals were similar to those reported in the literature and attributed to Cu(II) species.[12] The Cu(II) signals appeared from the very beginning of the polymerization and developed slowly afterward. This indicates that the equilibrium between the dormant species (most are the initiator molecules at this stage) (RBr) and the propagating radical (most are the initiator radicals) (R$^•$) was established very quickly:

$$RBr + Cu(I)Br \rightleftarrows R^• + Cu(II)Br_2 \qquad (1)$$

Take MMA/EGDMA (94.2/5.8 mol/mol) as an example. Figure 2a shows the Cu(II) concentration profile. The starting Cu(II) concentration was about 8.7×10^{-4} mol/L. The Cu(I) content that was initially charged to the ampule was about 9.4×10^{-2} mol/L. About 0.93% of the Cu(I) species were converted to Cu(II) very quickly. According to the equilibrium, an equal molar (to Cu(II)) of radicals should be generated. But there were no radical signals of any kind in the ESR spectra in the early stage of the polymerization. This indicates that the radical concentration at this stage was below the limit of the ESR sensitivity ($\sim 10^{-7}$ mol/L). The difference between the Cu(II) and radical concentrations was caused by radical termination prior to the establishment of the equilibrium at the very beginning of the polymerization.

There are two possible fates for the radicals R$^•$: they are either terminated with each other permenantly, $k_t[R^•][R^•]$, or deactivated with $Cu(II)Br_2$ to become dormant, $k_d[R^•][CuBr_2]$. These two reaction rates are in competition. At the very beginning when there were no Cu(II) species present, the termination dominated. When an adequate Cu(II) concentration was generated, the deactivation rate approached that of activation, $k_a[RBr][CuBr]$. The equilibrium between the dormant and radical species was thus established. At this time, the ratio of the deactivation/termination rates, $k_d[R^•][CuBr_2]/k_t[R^•][R^•]$, increased to a level that effectively suppressed the radical consumption by termination. This initial equilibrium was most likely accomplished by the initiator radicals, i.e., the radicals without monomer addition yet. In this experiment, less than 1% of the initiator molecules was consumed for the equilibrium.

When the polymerization proceeded, the radical signals started to appear at about 170 min (in the 94.2/5.8 mol/mol 70 °C run). These signals, as well as all the others having different MMA/EGDMA compositions in this work, were identical to those observed in the conventional free-radical polymerization of MMA/EGDMA initiated by 2,2′-azobis(2-methylpropionitrile) (AIBN).[13] The spectra had a nine-line hyperfine structure (relative intensities: inner four lines 1, 3, 3, 1 and outer five lines 1, 4, 6, 4, 1) assigned to the methacrylate radicals trapped in a glassy polymer matrix.[14,15] In contrast, the methacrylate radicals in a more liquid environment such as monomer and/or solvent would have a 13-line hyperfine structure (inner eight 1, 1, 3, 3, 3, 3, 1, 1 and outer 1, 4, 6, 4, 1).[14,15] The appearance of the radical signals elucidates the involvement of the radical intermediates in the ATRP. It offers a strong support to the radical mechanisms originally proposed for the process.[5,6,11]

Characteristics of Cu(II)/Radical Concentration Profiles. The Cu(II) and methacrylate radical concentration profiles shown in Figure 2a can be divided into three definable stages. In the first stage, the increase of Cu(II) concentration was mild but continuous. The radical concentrations were too low to be detected by ESR ($<10^{-7}$ mol/L). The continuous increase of the Cu(II) concentration indicates a continuous process of radical termination. During this period of time, about 10^{-3} mol/L of Cu(II) species was newly generated, and thus an equal molar (to Cu(II)) of radicals was terminated. These radicals were most likely short-chain polymeric species, rather than the initiator moieties, considering that the time span of 2 h was adequate to allow the addition of monomer molecules to individual chains. The change of the radical concentration during this stage was unknown. According to the equilibrium

$$PBr + Cu(I)Br \rightleftarrows P^• + Cu(II)Br_2 \qquad (2)$$

an increase of the Cu(II) concentration should correspond to a decrease of the radical concentration, if the equilibrium constant remained unchanged; i.e., the reactions were chemically controlled. The radical concentration could also increase if the equilibrium constant experienced an increase due to a mild diffusion control in the radical deactivation. The equilibrium constant K_{eq} in this work is defined as the ratio of the rate constants of radical activation over deactivation k_a/k_d. It equals $([P^•][CuBr_2])/([PBr][CuBr])$ when the reactions are in equilibrium:

$$K_{eq} = k_a/k_d = ([P^•][CuBr_2])/([PBr][CuBr]) \qquad (3)$$

In the second stage, the Cu(II) concentration increased dramatically. The radical signals also started to appear during this stage. The radical signals grew very rapidly. This phenomenon is similar to the Trommsdorff effect in the conventional free radical polymerization of methacrylates, which is caused by a diffusion-controlled radical termination.[16] At high polymer concentration, polymer chains are entangled with one another. The radical termination becomes diffusion-

controlled with its rate severely reduced. At the same time, the radical species are continuously being generated through initiation. The radical population accumulates. In ATRP, the dramatic increase in the Cu(II) concentration and the appearance and growth of the methacrylate radical signals during the second stage strongly suggest a diffusion-controlled polymerization mechanism.

The Cu(II) species are generated by the activation reaction and consumed by the deactivation reaction assuming no side reactions, i.e.

$$d[CuBr_2]/dt = k_a[PBr][CuBr] - k_d[P^\bullet][CuBr_2] \quad (4)$$

There were only two possible explanations for the observed increase in the Cu(II) concentration, i.e., increase in the activation rate $k_a[PBr][CuBr]$ and/or decrease in the deactivation rate $k_d[P^\bullet][CuBr_2]$. The concentration product [PBr][CuBr] decreased because both [PBr] (= $[MBPA]_0 - [CuBr_2]$) and [CuBr] (= $[CuBr]_0 - [CuBr_2]$) decreased according to the mass balances where $[CuBr]_0$ and $[MBPA]_0$ are the initial concentrations of copper bromide and methyl α-bromophenylacetate, respectively. On the other hand, the concentration product $[P^\bullet][CuBr_2]$ increased. The increase in the activation rate constant k_a was unlikely because the polymerization temperature was well controlled and kept constant. The decrease in k_d was the only reason for the increase in the Cu(II) concentration, which meant a diffusion-controlled deactivation.

The mass balance of the radical population is governed by

$$d[P^\bullet]/dt = k_a[PBr][CuBr] - k_d[P^\bullet][CuBr_2] - k_t[P^\bullet][P^\bullet] \quad (5)$$

Termination is particularly sensitive to the radical concentration; it is a second-order reaction. The increase of the radical concentration also suggests that termination is diffusion-controlled.

In the third stage, the Cu(II) concentration leveled off while the radical concentration increased continuously but more gradual increase until it leveled off. The final Cu(II) concentration reached 7.5×10^{-3} mol/L in the MMA/EGDMA 94.2/5.8 mol/mol run, which counted for 8% of the Cu atoms initially charged to the polymerization system. The final radical concentration was 8.4×10^{-5} mol/L. The difference between the Cu(II) and radical concentrations meant the concentration of the terminated primary chains 7.4×10^{-3} mol/L (= $7.5 \times 10^{-3} - 8.4 \times 10^{-5}$). At the same time, the concentration of the dormant chains was 8.7×10^{-2} mol/L (= $9.4 \times 10^{-2} - 7.5 \times 10^{-3}$), comprising 92% of the total chain population. The primary chains in the polymer network are those with the dimethacrylate cross-linkages severed.

Figure 2b shows the change of the equilibrium constant calculated by

$$K_{eq} = ([P^\bullet][Cu^{II}])/(([MBPA]_0 - [Cu^{II}])([CuBr]_0 - [Cu^{II}])) \quad (6)$$

The K_{eq} values in the early stage were unknown. The literature data[1] were on the order of 10^{-8}. The constant experienced more than 3 orders of magnitude rise during the polymerization.

Diffusion-Controlled Radical Deactivation and Termination. The radical deactivation rate constant can be expressed as

$$1/k_d = 1/k_{dC} + 1/k_{dD} \quad (7)$$

where the subscripts "C" and "D" indicate "chemically controlled" and "diffusion-controlled", respectively. Under the isothermal condition, the k_{dC} value remains constant. However, k_{dD} is proportional to the diffusion coefficients of the reactants—a propagating radical chain and the $CuBr_2$/HMTETA complex.[17] Compared to the complex molecule, the radical chain has a larger molecular size particularly at high conversions and thus is slower in diffusing. The diffusion-controlled deactivation rate is therefore determined by the diffusion of the complex. In the first stage, the system has low polymer concentration and polymer molecular weight. The complex molecules move fast, and the k_{dD} value is much higher than that of k_{dC} so that k_d is unaffected by k_{dD}. At the onset of stage two, both polymer concentration and molecular weight increase to a level that the system becomes viscous, and the complex molecules start to experience diffusion limitations. The k_{dD} value becomes comparable with k_{dC} (in the magnitude of 10^7 M^{-1} s^{-1}), and the k_d value starts to decrease. When the polymerization proceeds further to higher conversions, particularly in a network formation system, the diffusion of the complex molecules is severely restricted, resulting in a dramatic decrease in k_{dD} (i.e., a dramatic increase in $1/k_{dD}$). The deactivation reaction becomes totally diffusion-controlled with the term $1/k_{dC}$ contributing little to the $1/k_d$.

The diffusion control affects the fast reaction first. Compared to the deactivation, the radical activation reaction also involves a chain species (PBr) and a complex (CuBr/HMTETA). The k_{aD} in $1/k_a = 1/k_{aC} + 1/k_{aD}$ and the k_{dD} in $1/k_d = 1/k_{dC} + 1/k_{dD}$ are approximately equal because of the similar sizes of the Cu(I) and Cu(II) complex molecules. However, k_{aC} is in the range of 10^{-1}−1 M^{-1} s^{-1}, which is more than 7 orders of magnitude lower than k_{dC}. Therefore, the diffusion control in k_a comes much later than that of k_d. For example, when k_{aD} (and k_{dD}) = 10^5 M^{-1} s^{-1}, the deactivation becomes diffusion-controlled with $k_d \approx k_{dD} = 10^5$ M^{-1} s^{-1} while the activation remains unaffected. From the following equation

$$K_{eq} = k_a/k_d = (k_{aC}/k_{dC})(k_{aD}/k_{dD}) \times ((k_{dC} + k_{dD})/(k_{aC} + k_{aD})) \quad (8)$$

the equilibrium constant K_{eq} increases from k_{aC}/k_{dC} to k_{aD}/k_{dD} (≈1) at the extreme. The final K_{eq} in the MMA/EGDMA 97/3 run, as shown in Figure 2b, approached 10^{-4}, indicating that $k_d \approx k_{dD}$ was in the range of 10^3−10^4 M^{-1} s^{-1} and k_a was still chemically controlled.

Radical termination is most vulnerable to diffusion control because both reactants are chain species, which could readily experience diffusion limitations due to severe chain entanglements particularly in a network-forming system. The diffusion coefficient of chain species in a polymer matrix can be described either by the reputation theory, $D_p \sim M^{-2}C_p^{-7/4}$ where M is the chain molecular weight and C_p is the polymer concentration,[18] or the free volume theory, $D_p \sim M^{-\alpha} \exp(-\beta/v_f)$ where $\alpha = 0.5-2.5$, $\beta = 0.5-1.5$, and v_f is the free volume that can be related to the polymer concentration.[19] The

strong dependence of the diffusion coefficient on the polymer molecular weight and concentration is evident from the exponential factors. At high conversions, the diffusion of a whole polymer chain virtually stops. The radical center migrates through propagating with monomer molecules—the so-called "propagation diffusion" ($D_p \sim k_p[M]$) which depends on the diffusion of monomer molecules.[20] In the third stage of polymerization as shown in Figure 2A, the continuous increase in the radical concentration may be caused by the diffusion-controlled propagation.

The ATRP process suffers a severe loss of its livingness because of the diffusion-controlled radical deactivation. The radicals are uncapped and are thus not protected from termination due to their high concentration and to the second-order nature of the termination reaction. The diffusion-controlled deactivation also damages the control over polymer molecular weight development. The radicals are much longer lived with too many monomer molecules possibly added between successive capping events. In contrast, the diffusion-controlled radical termination promotes the process livingness. The combined effects of the diffusion-controlled deactivation and termination on the ATRP process depend on the relative levels of the diffusion limitations experienced by the respective reactants. The molecular sizes of monomer, catalyst/ligand complex, and various chain species determine the onsets of the diffusion-controlled reactions. A small catalyst/ligand complex would be preferred for delaying the diffusion-controlled deactivation.

Effect of EGDMA Level on Cu(II) and Radical Concentrations. Figure 3a shows the Cu(II) concentration profiles at six levels of EGDMA fraction—5.8, 9.5, 14.8, 18.2, 26.1, and 33.3 mol % on the vinyl basis (very close to the weight basis), which is equivalent to 3, 5, 8, 10, 15, and 20 mol % on the molecular basis (note: an EGDMA molecule has two vinyl groups). The absolute Cu(II) concentrations at 46.2 and 66.7 mol % vinyl EGDMA (30 and 50 mol % molecular) were not estimated due to the lack of Cu(II) reference spectra free of the methacrylate radical signals which appeared immediately at the start of polymerization. Figure 3a shows that the initial Cu(II) concentrations were almost the same with different EGDMA levels, about 10^{-3} mol/L. The Cu(I) concentrations initially charged were also very close, about 10^{-1} mol/L. (They were precisely 0.094, 0.0945, 0.0952, 0.0956, 0.0966, 0.0974, 0.0989, and 0.102 mol/L, corresponding to the eight EGDMA levels to remain [vinyl of MMA/EGDMA]/[MBPA]/[CuBr]/[HMTETA] = 100:1:1:1.) About 1% Cu(I) atoms were oxidized to Cu(II) for establishing the initial equilibria regardless of the comonomer composition.

The EGDMA level had a strong effect on the onset of the diffusion-controlled radical deactivation. The higher the EGDMA fraction, the earlier the deactivation became diffusion-controlled. This was because the higher EGDMA level made the system gelled quicker. For the same reason, the radical signal appeared earlier in the runs with higher EGDMA levels. Figure 3b,c gives the corresponding methacrylate radical concentration profiles. The onset time of the radical signal appearance is plotted against the EGDMA fraction in Figure 4. It took 171 min for 5.8 mol % EGDMA while only 7 min for the 66.7 mol % EGDMA.

The EGDMA level also had a strong effect on the final Cu(II) and radical concentrations. Figure 5 shows the relationship between the concentrations and the EGDMA fraction. The higher EGDMA fraction yielded higher [Cu(II)] and [P•]. At this final stage of polymerization, the system was fully gelled. The Cu(II) and radical species were trapped in the network. The higher the EGDMA level, the higher the cross-link densities and the more rigid the network. The trapped radicals were long-lived and could be terminated either by elevating temperature or exposing the sample to air.

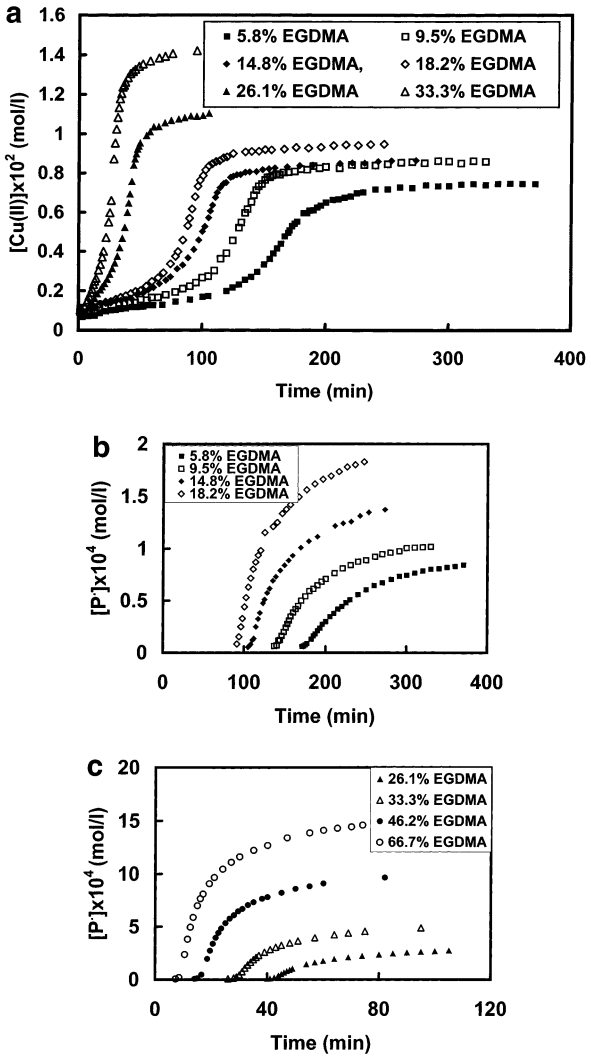

Figure 3. (a) Cu(II) concentrations and (b, c) radical concentration profiles of the ATRP of MMA/EGDMA. [MMA/EGDMA]/[MBPA]/[CuBr]/[HMTETA] = 100/1/1/1 (vinyl based mol/mol), 70 °C. The vinyl-based EGDMA mole fractions are as indicated.

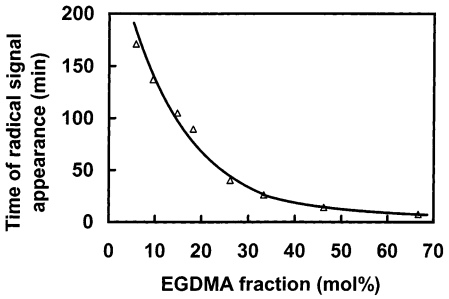

Figure 4. Time at which the methacrylate radical first appeared in the ATRP of MMA/EGDMA. See Figure 3 for the experimental conditions.

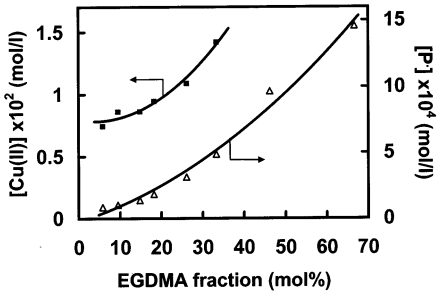

Figure 5. Cu(II) and radical concentration trapped at the final stage of the ATRP of MMA/EGDMA as a function of EGDMA fraction. The experimental conditions are same as in Figure 3.

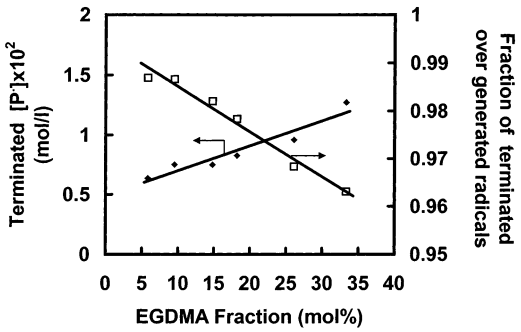

Figure 6. Terminated radical concentration and ratio of terminated over generated radical concentrations at the final stage of the ATRP of MMA/EGDMA as a function of EGDMA fraction. The experimental conditions are the same as in Figure 3.

The difference between the Cu(II) concentration and that of radicals is the concentration of terminated radicals, $[Cu^{II}] - [P^{\bullet}]$ (equivalent to the concentration of dead chains). Figure 6 shows that the terminated radical concentration at the final stage increased with the EGDMA level. This is because the more rigid network imposed more severe diffusion limitations to the Cu(II) complex molecules so that more radicals were uncapped and terminated. At the same time, the more rigid network also trapped more radicals which made the fraction of the terminated radicals over the total generated (equal to $[Cu^{II}]$) decrease with the EGDMA level.

Effects of Catalyst Concentration, Initiator Concentration, and Temperature. Figure 7a,b shows the Cu(II) and radical concentration profiles for the three levels of initially charged CuBr/HMTETA. The [MMA]/[vinyl of EGDMA]/[MBPA] was 81.8/18.2/1 in molar and remained the same for the three runs. The [CuBr]/[HMTETA] also remained 1/1 mol/mol. The [CuBr/HMTETA]/[MBPA] varied from 0.5, to 1.0, to 2.0. Doubling the catalyst concentration made the onset of diffusion control earlier. The reason for this is that more CuBr molecules generated more Cu(II) species and more radicals. The polymerization rate thus increased and the system gelled earlier. Reducing the catalyst amount to half of the initiator slowed the polymerization rate and postponed the diffusion-controlled reaction.

Figure 8a,b shows the dependence of initiator concentration. The [MMA]/[vinyl of EGDMA]/[CuBr]/[HMTETA] of 81.8/18.2/1/1 remained unchanged with the [MBPA]/[CuBr] varying from 0.5, to 1, to 2. Increasing the initiator concentration delayed the onset of diffusion control. The higher initiator concentration was expected to generate more radicals and to promote the polymerization rate so that the system gelled earlier and was therefore diffusion-controlled. Examination of the Cu(II) concentrations at the early stage of polymerization revealed that the starting Cu(II) concentrations were higher with the higher initiator concentrations. However, the increase in [Cu(II)] was slower. An explanation is that increasing the initiator concentration decreased the polymer chain lengths. The diffusion limitations were milder because of the diffusing radical species had shorter chains and also because of the polymer matrix consisted of shorter chains. The system gelled later because of the shorter chains. Once gelled, the network was not as rigid. The radical termination was more significant. The final radical concentration was therefore lower as shown in Figure 8b.

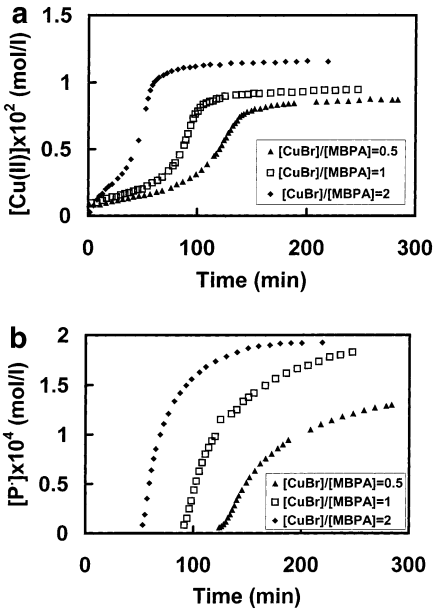

Figure 7. (a) Cu(II) concentration and (b) radical concentration profiles with different catalyst concentrations. The ratio of [MMA]/[EGDMA]/[MBPA] = 81.8/18.2/1 mol/mol vinyl. [CuBr]/[HMTETA] = 1/1 (mol/mol), 70 °C. The [CuBr]/[MBPA] ratios are as indicated.

Figure 9a,b shows the Cu(II) and radical concentration profiles for the [MMA]/[vinyl of EGDMA]/[MBPA]/[CuBr]/[HMTETA] of 81.8/18.2/1/1/1 system at 70, 80, and 90 °C. Elevating the reaction temperature increased the initial Cu(II) concentration, indicating that the radical activation reaction has a higher activation energy than that of the radical deactivation. The polymerization rate increased with the temperature and the system gelled earlier so that accelerated the onset of the diffusion control. The radical concentrations were lower at the higher temperatures. At 90 °C, the radical concentration decreased in the final stage, indicating a continuous termination process. This could be attributed either to the diffusion of radical centers through the monomer propagation (the "propagation diffusion"[20]) or to the relaxation of the polymer network at the high temperature. The final Cu(II) concentrations increased with the elevation of temperature, probably due to the more significant radical termination that moved the equilibrium from Cu(I) to Cu(II).

A basic question concerned what factors determined the onset of the diffusion control. The monomer conversion and the gel fraction data were measured at the time of the radical signal appearance for different EGDMA levels. The onset-point monomer conversion was about

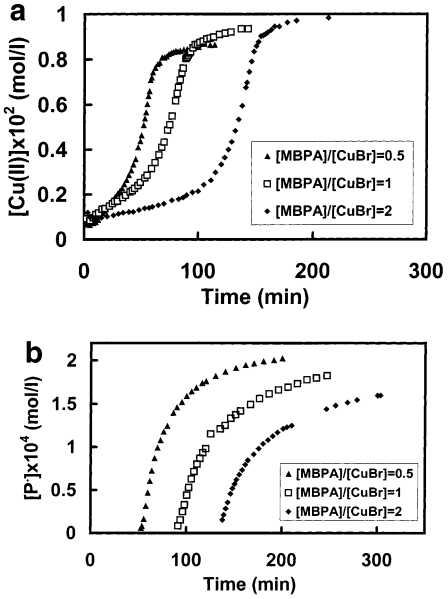

Figure 8. (a) Cu(II) concentration and (b) radical concentration profiles with different initiator concentrations. The ratio of [MMA]/[EGDMA]/[CuBr]/[HMTETA] = 81.8/18.2/1/1 mol/mol vinyl, 70 °C. The [MBPA]/[CuBr] ratios are as indicated.

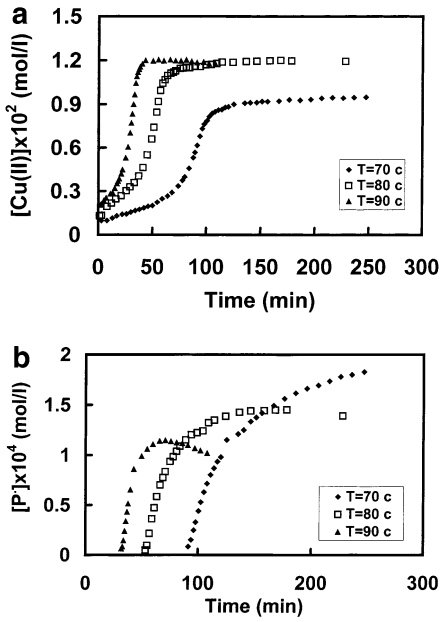

Figure 9. (a) Cu(II) concentration and (b) radical concentration profiles with different polymerization temperatures. [MMA]/[EGDMA]/[MBPA]/[CuBr]/[HMTETA] = 81.8/18.2/1/1/1 (mol/mol vinyl). The temperatures are as indicated.

90% at the EGDMA level of less than 18.2 mol % and decreased to about 50% at the 46.2% EGDMA. However, the gel fractions at the onset points all reached almost 100%. The data suggest that the diffusion-controlled reactions were mainly caused by the network formation of the polymerization system. Once the system gelled, the polymer network imposed severe limitations to the diffusion of such reactants as monomer and catalyst/ligand molecules. The radical centers were attached to the network structures through the cross-linking of the dimethacrylate monomers.

Conclusion

Based on the experimental investigation of the ATRP of MMA/EGDMA system using the on-line ESR technique and the analysis of the collected data, the following conclusions are reached.

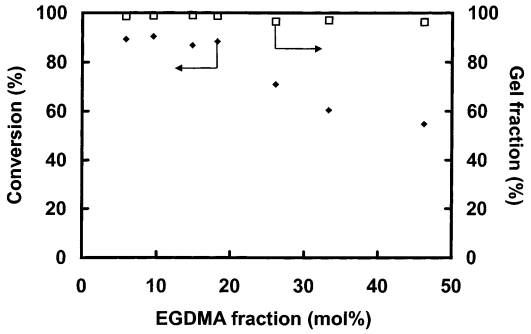

Figure 10. Gel fraction and monomer conversion at the time when the radical signals became detectable. The experimental conditions are the same as in Figure 3.

(1) The Cu(II) ESR signals were observable from the very beginning of the polymerization, while the radical signals appeared at the later stage. The signals were typical nine-line spectra assigned to methacrylate radicals. The appearance of the methacrylate radical signals supported the radical mechanisms proposed to the ATRP process. The absence of the signal at the early stage was because of the radical concentration lower than the ESR detectable limit (about 10^{-7} mol/L).

(2) The Cu(II)/radical concentration profiles had three definable stages. In the first stage, the Cu(II) concentration increased gradually, but no radical signals were observed. In the second stage, the Cu(II) concentration increased dramatically and the radical signal started to appear and increased quickly. In the third stage, the Cu(II) concentration leveled off while the radical concentration leveled off after some further increase.

(3) We believe the dramatic increase of the Cu(II) concentration and the appearance of the radical signal were caused by the diffusion-controlled radical deactivation and termination reactions. The network formation nature imposed severe limitations for the diffusion of the catalyst/ligand complex molecules. The radical centers were bounded to the network structure through the cross-linking of dimethacrylate monomers. The radical reactions readily became diffusion-controlled because their chemical activation rate constants were high. The diffusion control affected the fast reactions first. This diffusion-control work has implications for the control of ATRP at high monomer conversions.

(4) The onset of the diffusion control as well as the final Cu(II)/radical concentrations strongly depended on the EGDMA level. Increasing the EGDMA level accelerated the gelation and yielded more rigid networks and thus increased the Cu(II) and trapped radical concentrations. The Cu(II)/radical concentration profiles were also affected by the concentrations of catalyst/ligand and initiator as well as temperature. Increasing catalyst concentration and temperature accelerated the onset of diffusion control, while increasing initiator concentration delayed the onset.

Acknowledgment. The authors thank Prof. Youqing Shen, University of Wyoming, for his assistance in the sample preparation and helpful discussions. They also thank the Natural Science and Engineering Research Council of Canada (NSERC) for the financial support of this work.

References and Notes

(1) Matyjaszewski, K. *Chem. Rev.* **2001**, *101*, 2921.

(2) Kamigaito, M.; Ando, T.; Sawamoto, M. *Chem. Rev.* **2001**, *101*, 3689.
(3) (a) Szwarc, M. *Nature (London)* **1956**, *178*, 1168. (b) Szwarc, M. *J. Am. Chem. Soc.* **1956**, *78*, 2656.
(4) Georges, M. K.; Veregin, R. P. N.; Kazmaier, P. M.; Hamer, G. K. *Macromolecules* **1993**, *26*, 2987.
(5) Solomon, D. H.; Rizzardo, E.; Cacioli, P US Pat. 4,581,429, 1986.
(6) (a) Wang, J. S.; Matyjaszewski, K. *J. Am. Chem. Soc.* **1995**, *117*, 5614. (b) Matyjaszewski, K.; Wang, J. S. *Macromolecules* **1995**, *28*, 7901.
(7) Kato, M.; Kamigaito, M.; Sawamoto, M.; Higashimura, T. *Macromolecules* **1995**, *28*, 1721.
(8) Chiefari, J.; Chong, Y. K.; Ercole, F.; Krstina, J.; Jeffery, J.; Le, T. P. T.; Mayadunne, R. T. A.; Meijs, G. F.; Moad, C. L.; Moad, G.; Rizzardo, E.; Thang, S. H. *Macromolecules* **1998**, *31*, 5559.
(9) Hawthorne, D. G.; Moad, G.; Rizzardo, E.; Thang, S. H. *Macromolecules* **1999**, *32*, 5457.
(10) Yu, Q.; Zeng, F.; Zhu, S. *Macromolecules* **2001**, *34*, 1612.
(11) Matyjaszewski, K. *Macromolecules* **1998**, *31*, 4710.
(12) Kajiwara, A.; Matyjaszewski, K. *Macromol. Rapid Commun.* **1998**, *19*, 319.
(13) Zhu, S.; Tian, Y.; Hamielec, A. E.; Eaton, D. R. *Polymer* **1990**, *31*, 154.
(14) (a) Zhu, S.; Tian, Y.; Hamielec, A. E.; Eaton, D. R. *Macromolecules* **1990**, *23*, 1144. (b) Tian, Y.; Zhu, S.; Hamielec, A. E.; Eaton, D. R. *Polymer* **1992**, *33*, 384.
(15) Kamachi, M. *Adv. Polym. Sci.* **1987**, *82*, 207. (b) Kamachi, M. *J. Polym. Sci., Polym. Chem.* **2002**, *40*, 269.
(16) Trommsdorff, E.; Kohle, H.; Lagally, P. *Makromol. Chem.* **1948**, *1*, 169.
(17) Smoluchowski, M. *Z. Phys. Chem. (Munich)* **1918**, *92*, 129.
(18) de Gennes, P. G. *J. Chem. Phys.* **1971**, *55*, 572.
(19) Bueche, F. *Physical Properties of Polymers*; Interscience: New York, 1962.
(20) Stickler, M.; Panke, D.; Hamielec, A. E. *J. Polym. Sci., Polym. Chem. Ed.* **1984**, *22*, 2243.

MA0211277